Proceedings of the Eighth International Conference
on Engineering Computational Technology,
B.H.V. Topping, (Editor),
Civil-Comp Press, Stirlingshire, Scotland

Paper 109

Seismic Stability of Reinforced Soil Slopes

I. Tzavara[1], V. Zania[2], Y. Tsompanakis[1] and P.N. Psarropoulos[3]
[1] Department of Applied Sciences, Technical University of Crete, Greece
[2] Department of Civil Engineering
Technical University of Denmark, Kgs. Lyngby, Denmark
[3] Department of Infrastructure Engineering
Hellenic Air-Force Academy, Greece

Abstract

Over recent decades increased research interest has been observed on the dynamic response and stability issues of earth walls and reinforced soil structures. The current study aims to provide an insight into the dynamic response of reinforced soil structures and the potential of the geosynthetics to prevent the development of slope instability taking advantage of their reinforcing effect. For this purpose, a one-dimensional (SDOF) model, based on Newmark's sliding block model as well as a two-dimensional (plane-strain) dynamic finite-element analyses are conducted in order to investigate the impact of the most significant parameters involved, such as the flexibility of the sliding system, the mechanical properties of the soil and of the geosynthetics material, the frequency content of the excitation and the interface shear strength.

Keywords: seismic slope stability, geosynthetics, soil reinforcement, sliding, coupled SDOF models, finite-element analyses.

1 Introduction

Being a relatively inexpensive and abundant construction material, soil is ideal for various engineering applications, such as structure and infrastructure construction. Like other construction materials with limited tensile or shear strength, soil can be reinforced with other materials, such as metal strips, steel meshes and bar mats, geosynthetics and even bamboo, in the form of a composite material with increased strength. Nowadays, geosynthetic soil reinforcement is a widespread technique which is used to stabilize slopes, especially after a failure has occurred or if a steeper than a "safe" unreinforced slope needs to be constructed. Reinforced soil structures are also known as mechanically stabilized earth (MSE) structures. The design of geosynthetic reinforced slopes is based on modified versions of classical limit equilibrium slope stability methods. Kinematically, the potential failure surface in a reinforced homogenous slope is assumed typically to be defined by the same idealized geometry (but not location) as in the unreinforced case (for example circular, log spiral, bilinear wedge). Statically, the inclination and distribution of the reinforcement tensile force along the failure surface must be postulated. The capacity of reinforcement is taken as either the allowable pull-out resistance behind the potential failure surface, or as its allowable design strength, whichever is less. The target factor of safety for a reinforced slope is the same as for an unreinforced slope [1, 2].

In general, seismic stability of geosynthetic reinforced soil structures is being assessed via pseudo-static limit-equilibrium methods. These methods calculate dynamic earth pressures using the Mononobe-Okabe method or a modified two-part wedge method, which constitute essentially the same approach that has been used for many years for the stability analysis of conventional gravity retaining wall structures [3, 4]. In order to provide reasonable predictions of wall stability, empirical reductions of dynamic forces have often been employed [5, 6]. The so-called “displacement methods” or “permanent deformation analyses”, that treat the failed soil mass and gravity wall structure as separate rigid bodies have been proposed to overcome the non-compliance of limit-equilibrium based methods with observed performance in conventional gravity structures [4, 7, 8].

Newmark [9] suggested a relatively simple analytical model, in which the displacement of a soil mass above a slip surface is modelled as a rigid block of soil sliding on a plane surface. When the acceleration of the block exceeds the yield acceleration, a_y, the block begins to slide along the plane and the velocity of the block relative to the velocity of the underlying mass increases. This stick-slip pattern of motion continues until the acceleration falls below the yield acceleration and the velocity drops to zero. The computation of the permanent displacement is achieved by double integrating the relative acceleration. This methodology has been used by Richards and Elms [4] for gravity retaining walls. However, this method should be improved in order to introduce further complexities associated with geosynthetic reinforced slopes, such as rate dependency of polymeric reinforcements, or the tension and pull-out forces induced by the reinforcement [1, 10].

The abovementioned Newmark’s approach has been applied extensively for the seismic stability assessment of earth structures, even though the accuracy of the method is limited by the following assumptions: (a) the soil behaves in a rigid, perfectly plastic manner, (b) displacements occur along a single, well-defined slip surface, (c) the stress-strain behaviour of shear strength of interface is rigid-plastic, (d) the uphill resistance is infinitely large, (e) the input motion is horizontal, and (f) the sliding surface is plane. Among the most common applications of the sliding block model is the estimation of the seismic behaviour of rigid gravity [7, 11] or tie-back retaining walls [12], concrete gravity dams [13]. Ling [12] has also reported the application of the sliding-block theory to different geotechnical structures.

Nevertheless, the design procedures to evaluate earthquake-induced sliding displacements typically refer to three different approaches: (a) simplified dynamic analysis, by means of the conventional Newmark rigid block model, (b) dynamic analysis accounting for the flexibility of the oscillating mass, where the dynamic response and the sliding block displacements are computed separately, referred as decoupled approach, and (c) dynamic analysis where the dynamic response and slip displacement accumulation are considered simultaneously, commonly named as coupled analysis [14]. The latter has been substantiated by investigation of the response of SDOF lumped mass systems capable of considering simultaneously the dynamic response and development of displacements, which were also representative of seismic isolation systems [15, 16, 17]. Modal based solutions of systems with distributed mass and elasticity have been also reported [13], in which only the fundamental vibration mode shape was taken into account in order to calculate the response of a gravity dam. Furthermore, Lin and Whitman [18] have examined the dynamic response and the corresponding slip displacements using the coupled method for three MDOF lumped-mass systems, accounting for the effect of the depth of the failure wedge.

Except from analytical methods, centrifuge model studies have also been performed to investigate the response of reinforced soil structures due to dynamic loading. For instance, Nova-Roessig and Sitar [10] performed a series of centrifuge tests on reinforced slopes. The 48 models had a prototype height of 7.32m and 2V:1H face inclination. Each centrifuge test included two back-to-back slopes, one reinforced with L/H =0.7 and the other with L/H =0.9 (see Figure 1). The results of this study indicated that lateral displacements of a reinforced soil slope increase with: a) increase of input motion amplitude and duration, b) decrease of reinforcement length and stiffness, and c) decrease of backfill density.

In the current study the role of the seismic stability of reinforced soil slopes is examined and the permanent deformation accumulation is estimated via the application of two different approaches. Firstly, finite element analyses of a plane strain model based on the centrifuge model by Nova-Roessig and Sitar [10] are performed in order to investigate the ability of the geosynthetics to reduce the permanent deformation of the geostructure. The analysed model takes into consideration the effect of several important parameters, like the acceleration level, the interface properties, and the material properties of the geosynthetics. The results of the analyses demonstrate the effect of the magnitude of the induced acceleration on the accumulated plastic deformation and on the amplification of applied motion. On the other hand, simpler SDOF models were also developed with a sliding plane along their base, while the effect of the reinforcement was also taken into account, i.e., the failure plane and the stabilizing effect of the reinforcement were modelled. The dynamic response of the models to harmonic excitation was performed in accordance to the coupled procedure.

2 Plane-strain finite element modelling

The models developed for the numerical investigation in the current study are based on those used in the elaborate experimental study by Nova-Roessig and Sitar [10], which was conducted in order to provide a direct estimation of the impact of the geosynthetics. For this purpose, a series of dynamic centrifuge tests were performed on geosynthetic reinforced slopes and vertical walls reinforced with metallic mesh. Figure 1 presents the prototype model slope, which had a height of 7.3m and the inclination was set equal to 1H:2V, as it was materialised in the current study. Furthermore, eighteen sheets of reinforcement were required to maintain a static factor of safety of 1.5 when using a backfill with relative density of 75%. The length of the reinforcements did not strongly affect earthquake-induced deformations for values between 70%H and 90%H, which is typical of field conditions. Two slopes were placed back-to-back with enough unreinforced backfill between them to allow for the independent formation of potential failure surfaces. These slopes were called "north" (at the left slope, where the length of reinforcements was 90%H) and "south" (at the right slope, where the length of reinforcements was 70%H).

The dynamic finite element analyses of the present investigation were conducted utilizing ABAQUS software [19]. Figure 1b shows the finite element mesh of the prototype experimental configuration. The discretization of the backfill was performed using quadrilateral plane strain elements, the size (maximum length 0.5m) of which was tailored to the wavelengths of interest. The eighteen geosynthetic layers were placed as in the experimental setup. They were discretized with rod elements, since the geosynthetics are considered to attain only axial stiffness. The same material properties as in the experimental study were used. Hence, the axial stiffness of the geosynthetics was set equal to 8.3kN/m/m and the yield strength equal to 2.3kN/m^2. The elasticity modulus of the sand was set equal to 124MPa, leading thus to a shear wave velocity V_S equal to 170m/sec, while a Mohr Coulomb failure criterion was selected to represent the yield and plastic soil behaviour with angle of friction 42.5^o and angle of dilation 2^o. In order to ensure the stability of the symmetric slopes a small cohesion intercept was also applied, equal to 5kPa.

(a)

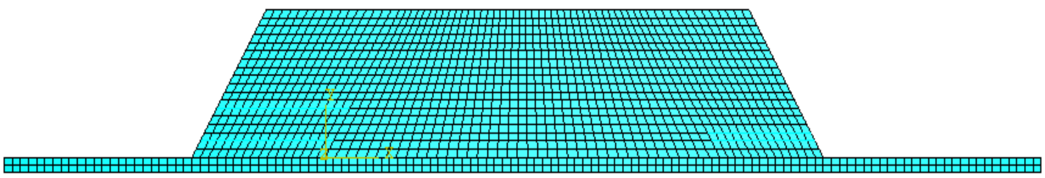

(b)

Figure 1: (a) Schematic representation of the developed finite element model. The 18 layers of reinforcement are shown in the south (right) and the north (left) slopes; (b) Finite element discretization of the examined model.

Dynamic analyses of the model were conducted using a horizontal input motion at the base of the model, i.e, a harmonic excitation with period T equal to 0.288 sec, as shown in Figure 2. The duration of the sinusoidal pulse was 1.728 sec and the applied motion was scaled to 3.924m/s^2(0.4g) and 7.848m/s^2(0.8g). The results in terms of permanent displacements are shown in Figure 3. The results of harmonic excitations are easier to understand, provide a clearer insight into the governing mechanisms, and are often used in dynamic analyses, especially in analytical calculations.

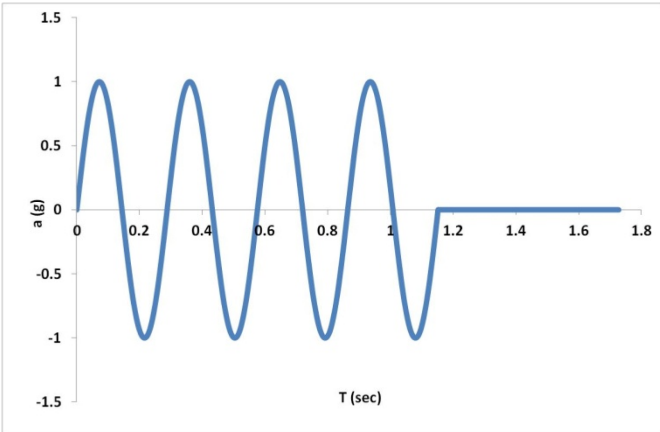

Figure 2: Normalized sinusoidal pulse used in the current study.

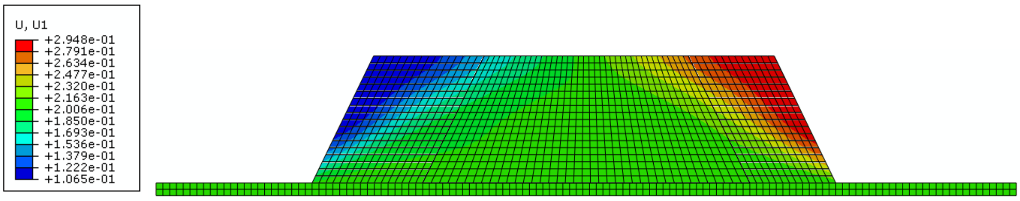

(a)

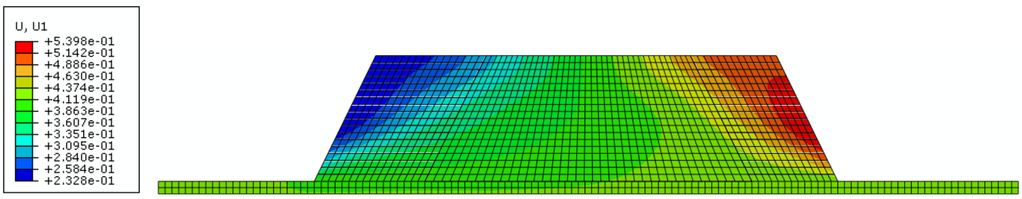

(b)

Figure 3: Contours of permanent horizontal displacements for maximum applied acceleration equal to: (a) 3.924 m/s^2, and (b) 7.848 m/s^2.

The permanent horizontal displacements at both north and south slopes appear to obtain a similar pattern when observing the contour plots for the two examined acceleration levels in Figure 3. The inclination of the failure zone does not seem to be drastically affected by the increase of the acceleration. This is further validated by the plastic shear strain contours shown in Figure 4. The plastic deformations are distributed in a wide zone, indicating also that a distinct failure surface is not formulated. The shape of the failure mass resembles closely to a triangular wedge. Moreover, the plastic strain time history of the south slope (node close to surface exposure of the yield surface) for the two examined acceleration levels are compared in Figure 5. It is evident that, the increase of the acceleration has resulted to increased cumulative plastic deformation per each cycle of applied motion and higher permanent deformation as well. The current observations are in qualitative agreement with the results of the experimental study [10]. In both studies it was found that the lower intensity motions are related to smaller horizontal deflections and that the reinforcement layers tend to spread out deformations throughout the reinforced zone and do not allow damage localization along a discrete failure surface. Hence, the assumptions of traditional limit equilibrium-based seismic design methods are not supported by the results of the experimental and the numerical investigation.

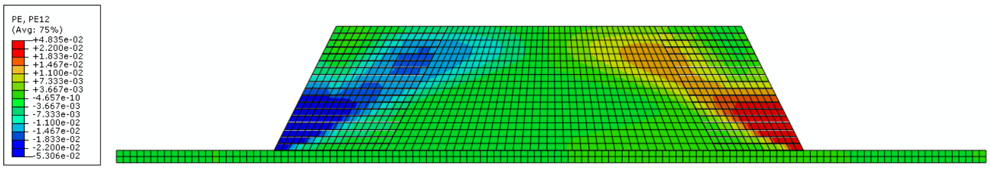

(a)

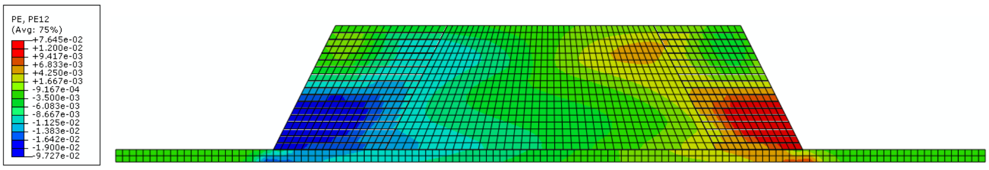

(b)

Figure 4: Contours of permanent plastic shear strain for maximum applied acceleration equal to: (a) 3.924 m/s^2, and (b) 7.848 m/s^2.

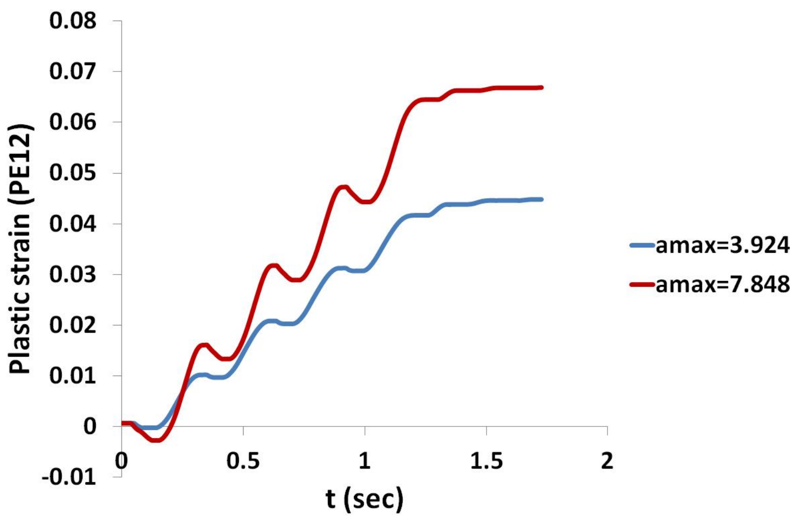

Figure 5: Time histories of plastic shear deformations accumulation for maximum applied acceleration equal to 3.924 m/s^2 and 7.848 m/s^2.

Moreover, it has been found that depending on the backfill density amplification occurs even for small to medium peak base accelerations, while de-amplification occurs at greater amplitudes [10]. The amplification of the applied motion as calculated in the FEM analysis is illustrated in Figure 6, where the acceleration time history of both the slope tip and the slope crest of the south slope are plotted for the two acceleration levels. Amplification of the induced acceleration is observed only for the case of lower maximum acceleration, while for higher acceleration levels the amplification is marginal. It appears also that the critical or yield acceleration is a factor of the maximum applied acceleration, being equal to the maximum applied acceleration for 0.4g and almost 75% of the maximum acceleration at 0.8g.

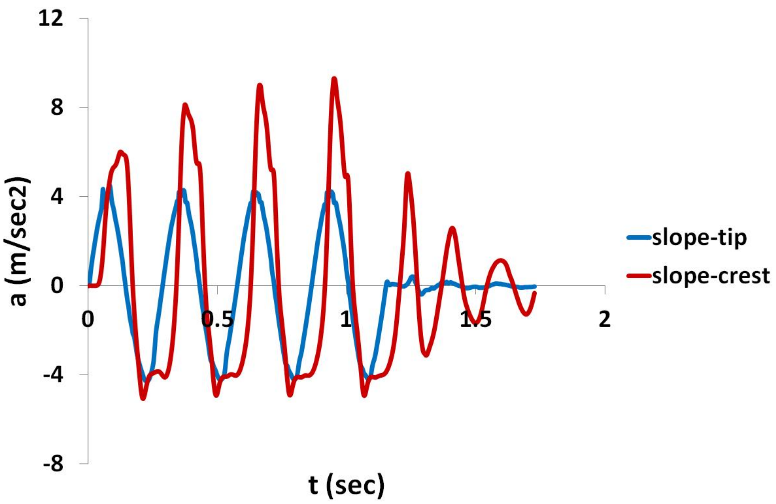

(a)

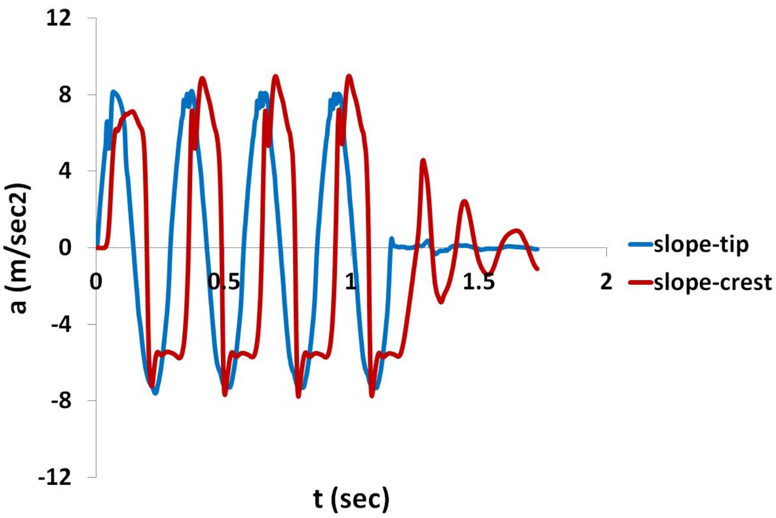

(b)

Figure 6: Acceleration time history at the lower right tip of the (south) slope and the top corner crest for maximum applied acceleration equal to: (a) 3.924 m/s^2, and (b) 7.848 m/s^2.

3 Lumped- mass SDOF model

The aforementioned experimental configuration was replicated as closely as possible herein utilizing a simplified lumped mass model, however, a full comparison was difficult to be performed and is also beyond the scope of this preliminary investigation. The prototype unreinforced model that has been used as reference for this work was proposed by Westermo and Udwadia [15]. Figure 7 illustrates the lumped mass SDOF shear beam model that has been developed in the current study. As it can be observed, the reinforced soil structure consists of five discrete parts, which are: (a) a concentrated mass (M), (b) a dashpot (coefficient c) and frictional interface, (c) beam element with stiffness (K), (d) a spring (with stiffness k) at the base to represent reinforcement, and (e) a gap element between the SDOF and the ground. The properties of the soil and the reinforcement were regarded constant, defined by the density ρ, the shear modulus G, Young modulus E and the Poisson's ratio v. These properties were taken from the experimental study by Nova- Roessig and Sitar [10].

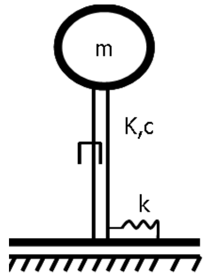

Figure 7: Illustration of the reinforced SDOF model and the discrete parts representing the inertia, elastic, damping, and reinforcement forces.

Parametric analyses of the developed coupled semi-analytical approach were performed utilizing the finite element software ABAQUS [19] that has been used to simulate the SDOF model shown in Figure 7. Furthermore, the reinforced model was investigated with a value of geosynthetics stiffness that directly affects the stiffness of the spring (k), which was equal to 8.3 kN/m/m (denoted as K_1). Since the dynamic response of the lumped mass model has been shown to be strongly dependent on two factors [20]: (a) the ratio of critical to maximum acceleration ($\tan\varphi * g/a_{max}$), and (b) the tuning ratio (denoted as $\beta=T_{str}/T$), which represents the ratio of the eigenperiod (T_{str}) of the structure to the period (T) of the excitation, the results are also interpreted referring to those ratios herein.

The present coupled formulation allows the calculation of the sliding and permanent displacement. The sliding displacement (denoted as d in the vertical axis of the subsequent plots), is defined as the difference between the displacement at the base of the deformable sliding mass and the ground displacement. It has to be noted that the base (i.e., the sliding plane) of the deformable mass is not inclined. A parametric analysis was performed, taking into account the factors that influence the flexibility of the system. For this purpose, the dynamic response has been assessed for several SDOF models with varying flexibility, by calculating different values for the tuning ratio (β) equal to 0.0, 0.2, 0.4, 0.6, 0.8, 1.0, 1.5 and 2.0, while for the ratio of critical to maximum acceleration ($\tan\varphi*g/a_{max}$) the values of 1.0 and 0.5 were considered.

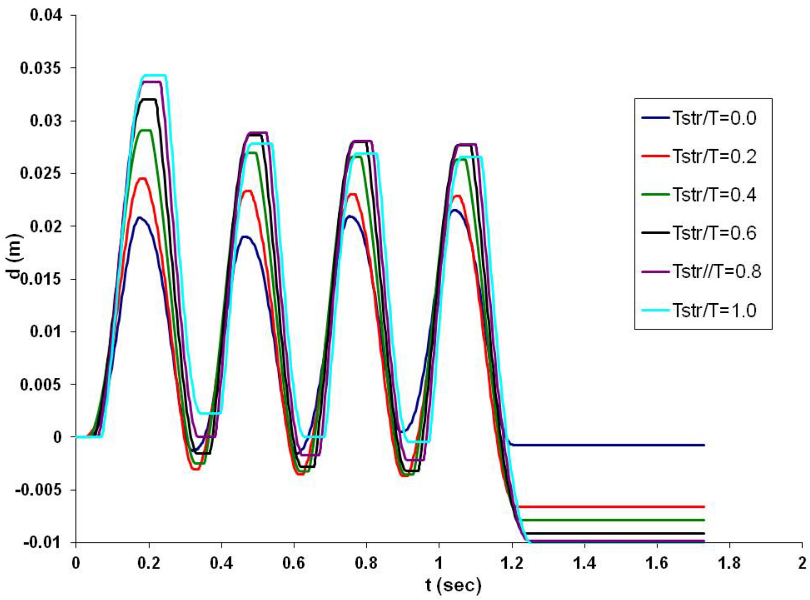

(a)

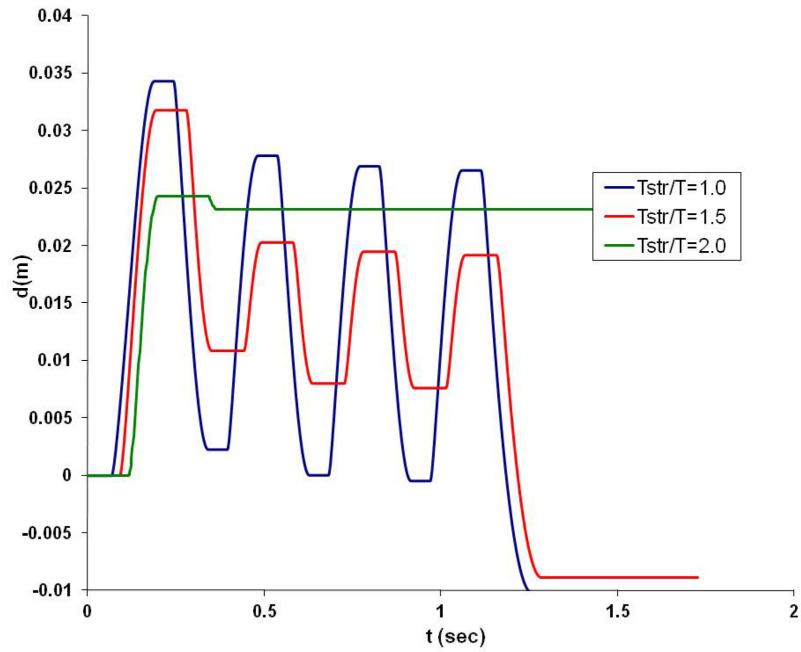

(b)

Figure 8: Accumulation of slip displacements for tuning ratio (β) equal to: a) 0.0, 0.2, 0.4, 0.6, 0.8, 1.0 and b) 1.0, 1.5, 2.0; while $\tan\varphi*g/a_{max}$ is equal to 0.5 and K_1 is equal to 8.3kN/m.

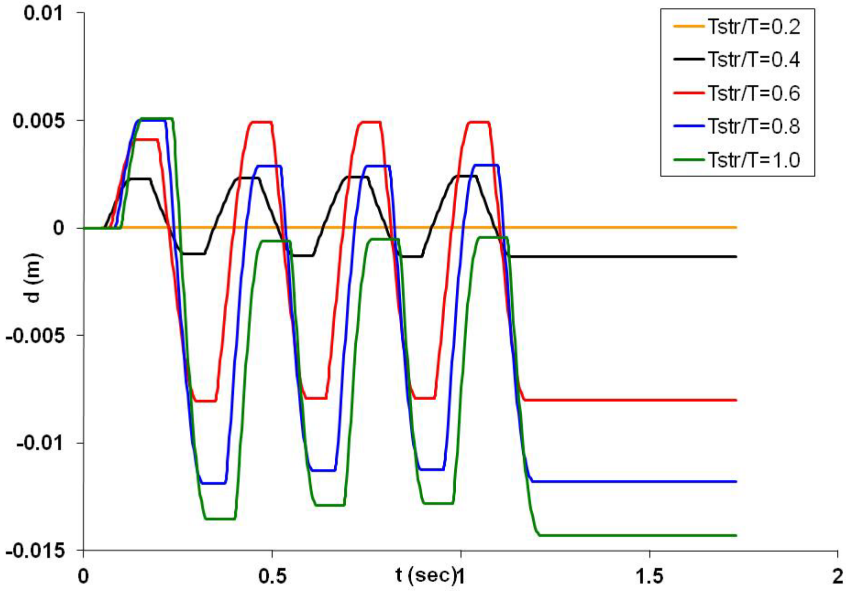

(a)

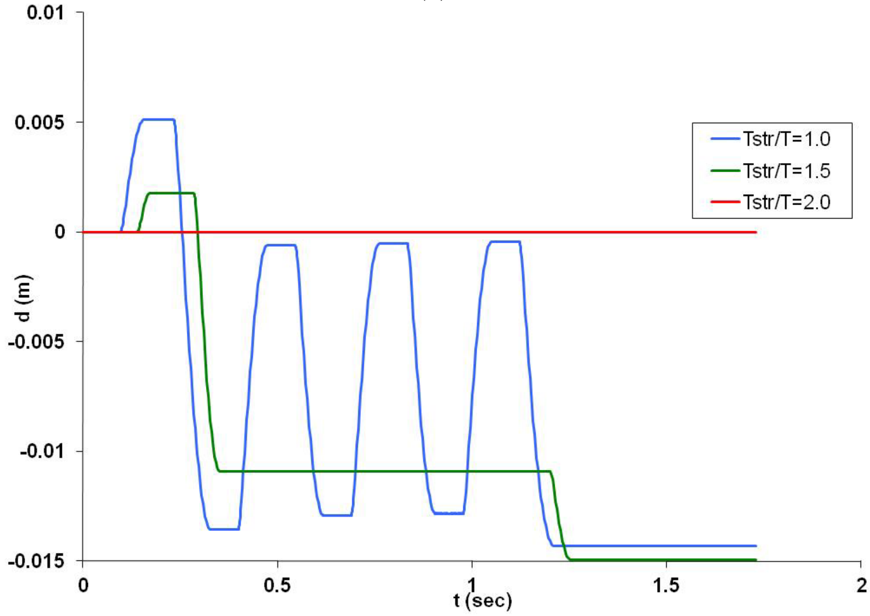

(b)

Figure 9: Accumulation of slip displacements for tuning ratio (β) equal to: a) 0.0, 0.2, 0.4, 0.6, 0.8, 1.0 and b) 1.0, 1.5, 2.0; while $\tan\varphi * g/a_{max}$ is equal to 1.0 and K_1 is equal to 8.3kN/m.

Figures 8 and 9 depict the time-histories of slip displacement accumulation of the SDOF model for tuning ratios equal to 0.0, 0.2, 0.4, 0.6, 0.8, 1.0 and 1.5, ratio $\tan\varphi * g/a_{max}$ equal to 0.5 (in Figure 8) and ratio $\tan\varphi * g/a_{max}$ equal to 1.0 (in Figure 9) and spring stiffness (k) equal to 8.3 kN/m/m. Results in Figures 8 and 9 show that for small tuning ratio values (β<1.0), increasing β leads to higher displacements, while the opposite trend occurs for ratios β>1.0. Note that in the first cycle of the input motion the calculated value of slip displacement is higher than the corresponding value during the second cycle, which affects the development of permanent displacements. Moreover, Figures 8 and 9 illustrate that the decrease of the ratio $\tan\varphi^*g/a_{max}$ (i.e., the increase of maximum acceleration) increases the slip and permanent displacements.

Finally, the impact of the yield acceleration ratio on permanent displacements was investigated, for ratio $\tan\varphi^*g/a_{max}$ equal to 0.5 and 1.0. The corresponding results are illustrated in Figure 10. It is evident that the increase of the yield acceleration ratio for values of tuning ratio lower than 0.6 resulted in an increase of the permanent displacements, while the opposite trend can be noticed for values of tuning ratio larger than 0.6.

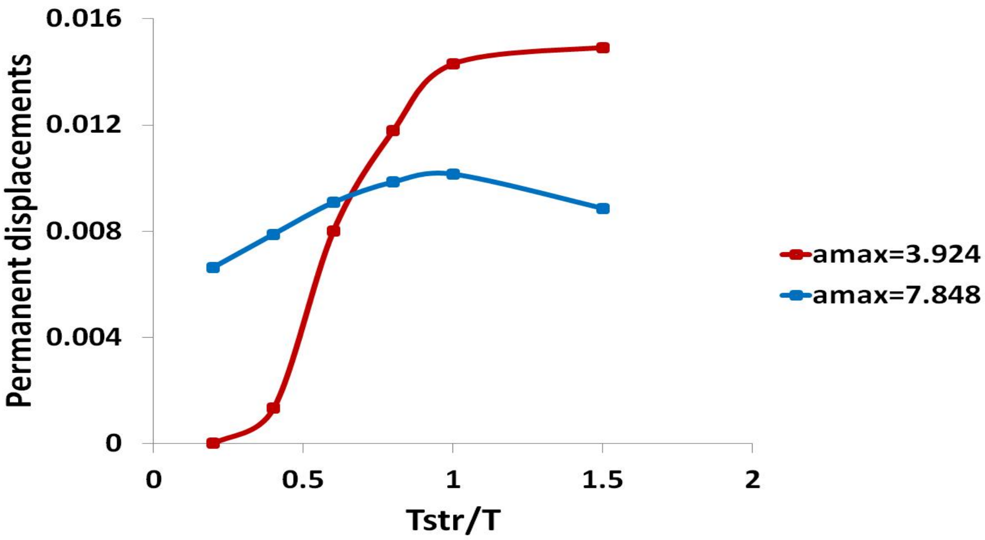

Figure 10: Coupled permanent displacements of a reinforced SDOF system with respect to the tuning ratio $\beta=T_{str}/T$, while the yield acceleration ratio ($\tan\varphi^*g/a_{max}$) is equal to 0.5 and 1.0.

3 Conclusions

In this paper, the seismic response of reinforced soil slopes was investigated focusing on the evaluation of instability in terms of permanent slip displacements. For this purpose, a two-dimensional finite-element simulation and a coupled SDOF semi-analytical model were formulated, which were subsequently used to calculate the magnitude of slip displacements. The coupled dynamic time history analyses which were performed took into account the flexibility of the sliding system, the mechanical properties of the soil and of the geosynthetic material. The general trends observed in the numerical results agree qualitatively with the corresponding ones derived from a series of geotechnical centrifuge tests of a previous study.

It is evident from the results that, as expected, the assumptions of traditional limit equilibrium-based seismic design methods are not supported by the findings of the experimental and the numerical investigations. In general, pseudo-static analyses cannot simulate the extensive (non-discrete) failure surfaces that develop in reinforced soil slopes and cannot estimate displacements. The critical failure surface predicted by pseudo-static analyses approximates only the region of significant deformations. By contrast, permanent deformation analyses can provide a realistic estimate of the developed displacements, but do not provide a distribution along the height of the earth structure. On the other hand, numerical methods (FE-based) can alleviate the deficiencies of the other two approaches, but provide satisfactory results only when proper interface simulation and advanced constitutive material modelling are used, which are not readily available.

The application of the two numerical approaches has illustrated the advantages and the shortcomings of each methodology. In any case, further research is required on further improvement of numerical simulations and sliding block methods to overcome their deficiencies and to capture as closely as possible the actual seismic performance of reinforced soil slopes.

Acknowledgements

This research has been co-financed by the European Union (European Social Fund - ESF) and Greek national funds through the Operational Program "Education and Lifelong Learning" of the National Strategic Reference Framework (NSRF) - Research Funding Program: Heracleitus II. Investing in knowledge society through the European Social Fund.

References

[1] S.B. Paulsen, “A Numerical Model for Estimating Seismic Displacements of Reinforced Steep Slopes”, MSc Thesis, University of Washington, 2002.

[2] L.W. Abramson, T.S. Lee, S. Sharma, and G.M. Boyce, “Slope stability and stabilization methods”, Wiley, 2002.

[3] H.B. Seed, and R.V. Whitman, “Design of earth retaining structures for dynamic loads”, ASCE Specialty Conference on Lateral Stresses in the Ground and Design of Earth Retaining Structures, Ithaca, NY, pp. 103-147,1970.

[4] R. Richards, and D.G. Elms, “Seismic behaviour of gravity retaining walls”, ASCE Journal of Geotechnical Engineering Division, 10.5(GT4), 449-464, 1979.

[5] B.R. Christopher, S.A. Gill, J.-P. Giroud, I. Juran, F. Schlosser, J.K. Mitchell, and J. Dunnicliff, “Reinforced soil structures - Volume I. Design and construction guidelines”, Federal Highways Administration, Washington USA, Report N_O. FHWA-RD-89-043, 1989.

[6] Reinforced Earth Company, "Reinforced Earth structures in seismic regions", Reinforced Earth Company Report, 1991.
[7] F. Nadim, and R.V Whitman, "Seismically induced movement of retaining walls", ASCE Journal of Geotechnical Engineering Division, 109(7), 915-931, 1983.
[8] J.-S. Lin, and R.V. Whitman, "Earthquake induced displacements of sliding blocks", ASCE Journal of Geotechnical Engineering Division, 112(1), 44-59, 1984.
[9] N.M. Newmark, "Effects of earthquakes on dams and embankments", Geotechnique, 15(2), 139-160, 1965.
[10] L.M. Nova-Roessig, and N. Sitar, "Centrifuge studies of the seismic performance of reinforced soil structures", Report No. UCB/GT/99-13, Dept. Civil Engineering and Environmental Engineering, University of California, Berkeley, USA, 1999.
[11] A.C. Trandafir, T. Kamai and R.C. Sidle, "Earthquake-induced displacements of gravity retaining walls and anchor-reinforced slopes", Soil Dynamics and Earthquake Engineering, 29, 428-437, 2009.
[12] H. Ling, "Recent applications of sliding block theory to geotechnical design", Soil Dynamics and Earthquake Engineering, 21, 189-197, 2001.
[13] A. Chopra and L. Zhang, "Earthquake-induced base sliding on concrete gravity dams", Journal of Structural Engineering, 117(12), 3698-3719, 1991.
[14] E. Ausilio, A. Constanzo and G. Tropeano, "Evaluation of seismic displacements of a natural slope by simplified methods and dynamic analyses in A. Kokusho, A. Tsukamoto and A. Yoshimine (Eds)", Performance-based design in earthquake geotechnical engineering, Taylor & Francis, London, pp. 955–962, 2009.
[15] B. Westermo and F. Udwadia, "Periodic response of a sliding oscillator system to harmonic excitation", Earthquake Engineering and Structural Dynamics, 11, 135-146, 1983.
[16] N. Mostanghel, M. Hejazi, J. Tanbakuchi, "Response of sliding structures to harmonic support motion", Earthquake Engineering and Structural Dynamics, 11, 355-366, 1983.
[17] M. Iura, K. Matsui and I. Kosaka, "Analytical expressions for three different modes in harmonic motion of sliding structures", Earthquake Engineering and Structural Dynamics, 21, 757-769, 1992.
[18] J.-S. Lin and R.V. Whitman, "Decoupling approximation to the evaluation of mearthquake-induced plastic slip in earth dams", Earthquake Engineering and Structural Dynamics 11, 667-678, 1983.
[19] ABAQUS, "Analysis User's Manual Version 6.8.2", ABAQUS Inc. USA, 2010.
[20] V. Zania, Y. Tsompanakis and P.N. Psarropoulos, "Seismic displacements of landfills and deformation of geosynthetics due to base sliding", Geotextiles and Geomembranes, 28, 491-502, 2010.